Geophysical Journal International

Geophys. J. Int. (2010) **183,** 1392–1400 doi: 10.1111/j.1365-246X.2010.04762.x

Inverse Common-Reflection-Surface

H. Perroud,[1] M. Tygel[2] and L. Freitas[3]

[1] *Université de Pau et des Pays de l'Adour, Pau, France. E-mail: herve.perroud@univ-pau.fr*
[2] *State University of Campinas - Unicamp, Campinas, Brazil*
[3] *Geoprocessados, Mexico*

Accepted 2010 August 4. Received 2010 July 1; in original form 2010 February 23

SUMMARY

The Common-Reflection-Surface (CRS) stack method is a powerful tool to produce high-quality stacked images of multicoverage seismic data. As a result of the CRS stack, not only a stacked section, but also a number of attributes defined at each point of that section, are produced. In this way, one can think of the CRS stack method as a transformation from data space to attribute space. Being a purely kinematic method, the CRS stack lacks amplitude information that can be useful for many purposes. Here we propose to fill this gap by means of a combined use of a zero-offset section (that could be a short-offset or amplitude-corrected stacked section) and common midpoint gather. We present an algorithm for an inverse CRS transformation, namely one that (approximately) transforms the CRS attributes back to data space. First synthetic tests provide satisfying results for the two simple cases of single dipping-plane and single circular reflectors with a homogeneous overburden, and provide estimates of the range of applicability, in both midpoint and offset directions. We further present an application for interpolating missing traces in a near-surface, high-resolution seismic experiment, conducted in the alluvial plain of the river Gave de Pau, near Assat, southern France, showing its ability to build coherent signals, where recording was not available. A somewhat unexpected good feature of the algorithm, is that it seems capable to reconstruct signals even in muted parts of the section.

Key words: Numerical approximations and analysis; Controlled source seismology.

1 INTRODUCTION

The Common-Reflection-Surface (CRS) stack method is a recent data-driven time imaging process (see, e.g. Hubral 1999; Jäger *et al.* 2001 and also references therein) that has been originally proposed as an alternative to the classical normal moveout (NMO)–dip moveout (DMO) chain (Yilmaz 2000) to build seismic stacked, simulated zero-offset (ZO) time images of the subsurface. As already discussed elsewhere (Perroud & Tygel 2005), the CRS stack method has both advantages and disadvantages with respect to its alternative approaches. In fact, the adoption of the CRS stack method by the geophysical community has been until now only limited, because the classical NMO-DMO chain already provides good-quality robust results, so the need for a change is not obvious.

However, the CRS stack method does not provide only ZO images, but also a set of wavefield attributes (also called CRS parameters: emergence angles and wave front curvatures) that have been exploited in several applications. These include, for example, velocity model building (Della-Moretta *et al.* 2001; Klüver 2006), multiple attenuation (Prüssmann *et al.* 2006) or residual statics correction (Koglin *et al.* 2006).

The CRS stack method can be seen as a transformation from the data space (seismic amplitudes as a function of position and time) into attribute space (wavefield attributes as a function of position and time). Note that data space position variables include both midpoint and offset coordinates, while the attribute space position variables consist in the midpoint coordinates only. In this way, the attribute domain is much smaller, even if several attributes exist per midpoint. This transformation can thus be represented by the equation

$$\{\mathcal{D}(t,m,h)\} \overset{\text{CRS}}{\Longrightarrow} \{\mathcal{P}(t,m)\}\,, \tag{1}$$

where $\mathcal{D}(t,m,h)$ and $\mathcal{P}(t,m)$ denote the data and attribute sets, respectively. Also, t denotes time, m midpoint position and h half-offset.

The CRS stack method provides also a generalized hyperbolic moveout expression that allows for traveltime estimations for a reflection event at any midpoint and offset in the vicinity of a reference position where the attributes have been estimated. In the simple situation considered here, that reference point is assumed to be a coincident source–receiver (ZO) point, which, in many cases, can be approximated by the midpoint of the shortest available source–receiver pair in the data. Moreover, to prove the concept, we also consider the 2-D situation and non-converted (say, *PP*) data. In this case, the number of CRS attributes is three. Assuming that these attributes, denoted by P_1, P_2 and P_3, were estimated at midpoint position

$m = 0$ and at time $t(0, 0)$, the traveltime, $t(m, h)$, for the same reflection event at the neighbouring midpoint m and half-offset h can be approximated as

$$t^2(m, h) = (t(0, 0) + P_1 m)^2 + P_2 m^2 + P_3 h^2 \,. \tag{2}$$

The traveltime of eq. (2) refers to a specific event (say, a primary reflection) from a single (target) reflector, which is, of course, not known. Following the literature (see, e.g. Jäger *et al.* 2001), the CRS attributes admit appealing geometric interpretations as angles and curvatures, related to the normal reflection (ZO) ray (called central ray) that connects the midpoint $m = 0$ (called central point) to the reflection point at the target reflector and then back to the central point. That reflection point is referred to as the *normal-incidence-point (NIP)*. More specifically, we have

$$P_1 = \frac{2 \sin \theta_0}{v_0}, \quad P_2 = \frac{2 t_0 \cos^2 \theta_0}{v_0} K_n, \quad P_3 = \frac{2 t_0 \cos^2 \theta_0}{v_0} K_{\rm nip} \,, \tag{3}$$

in which t_0 is the ZO time, v_0 is the medium velocity at the vicinity of the central point, and θ_0 is the emergence angle. Moreover, the quantities K_n and $K_{\rm nip}$ refer to the curvatures of the so-called *normal (N)* and *normal-incidence-point (NIP)* waves, respectively, at the emergence central point. As introduced in Hubral (1983), the N and NIP waves are fictitious *eigenwaves* with respect to the ZO central ray, which means that, for each of them, the wave fronts at the initial and endpoints of that ray coincide. The N and NIP waves differ by the behaviour of their wave fronts at the point NIP. In the vicinity of that point, the wave front of the N wave coincides with the reflector's curvature. On the other hand, the wave front of the NIP wave reduces to the NIP point. It is also instructive to observe that, for a common midpoint (CMP) gather around the central point ($m = 0$), the traveltime equation reduces to the well-known *normal moveout* (NMO) equation. As a consequence, the attribute P_3 can be readily interpreted as $P_3 = 4/v_{\rm nmo}^2$ where $v_{\rm nmo}$ is the usual NMO velocity. We remark, in passing, that a similar interpretation for P_2 as a velocity also exists (see, Hertweck *et al.* 2007).

The above representation of the data in the new (attribute) domain is not complete, since it is purely kinematic. We miss the amplitude of the seismic events, that are necessary for a full representation of the data. In this sense, it can be stated that the CRS transformation, on its own, induces a loss of information that cannot be reversed. To establish a transformation that could allow to go back from the attribute space to the data space, we need to add some dynamic information. Our purpose here is to demonstrate that this goal can be achieved if we have, in addition to the CRS attributes at a given trace, also data from two trace gathers in its vicinity. These are (1) the real-amplitude (as if measured) ZO gather and (2) the CMP gather centred at the reference midpoint. The chosen ZO and CMP traces should be sufficiently close to the reference midpoint, so that the validity of the CRS approximation of any reflection traveltime is valid in this range. We propose then to call this new transformation *Inverse CRS*. In symbols, it may be represented by the equation (compare with eq. 1)

$$\{\mathcal{P}(t, 0), \mathcal{D}(t, m, 0), \mathcal{D}(t, 0, h)\} \stackrel{\text{Inverse CRS}}{\Longrightarrow} \{\mathcal{D}(t, m, h)\} \,, \tag{4}$$

where $\mathcal{P}(t, 0)$ is the CRS attribute set at the reference midpoint, and $\mathcal{D}(t, m, 0)$ and $\mathcal{D}(t, 0, h)$ are the ZO and CMP data sets, respectively. Since the (forward) CRS transformation of eq. (1) is essentially an approximate process (namely, it is realized upon the use of the hyperbolic traveltime approximation 2), the proposed Inverse CRS transformation of eq. (4) should also not be expected to provide exact (loss-free) results. One of our goal is therefore to evaluate in which range these losses can be considered as insignificant.

It is to be remarked that a real-amplitude ZO section is not easily available in seismic exploration. As a consequence, to implement the CRS Inverse transformation, we need to assume that the ZO section is available. We remark, in passing, that the Inverse CRS transformation is not restricted to seismic data. For ground penetrating radar (GPR) data, for example, this drawback is overcome since a fairly close approximation to the ZO section can be obtained from measurements using shielded antennas. A discussion on how to obtain a valid approximation of the real-amplitude ZO section from the multicoverage data, that can be used for our Inverse CRS transformation purposes, lies outside the scope of this paper. Here we only observe that such ZO section can, in principle, be obtained together with the CRS attributes and an adequate average of the available, near-offset traces. An algorithm to actually perform this task is a topic of further investigation.

In the following, we describe the Inverse CRS transformation, as well as the algorithm that allows one to build a trace at any midpoint and offset. As indicated above, both the ZO and CMP sections in the vicinity of the reference trace are assumed to be available. For illustrative purposes, we apply it to two simple synthetic cases of a dipping planar and a circular reflector. Finally, our algorithm has been tested for the interpolation of missing traces in a real high-resolution seismic data set.

2 THE INVERSE CRS TRANSFORMATION

The problem to be solved can be formulated as follows: to build the unknown data trace at a given midpoint position and offset, in the vicinity of a reference trace, for which we know (1) the CRS attributes, (2) the ZO gather and (3) the CMP gather. The known ZO and CMP gathers consist of traces located in the vicinity of the reference trace.

The construction of the unknown data trace means filling the 'right' amplitude (i.e. a valid approximation of it) at all time samples. We therefore need to estimate both time and amplitude for all events that can be identified in the known part of the data. We shall describe below how these are estimated. As far as possible, we want this transformation to be macro-model independent, so we shall try to use in the process data-related quantities only.

2.1 Equation for traveltime

Traveltime estimation can be achieved directly using the CRS traveltime approximation, like the one shown above in eq. (2) for the 2-D case. For an event such that the ZO traveltime at the reference point is $t(0, 0)$, we can evaluate the corresponding traveltime at any neighbouring position m and half-offset h, since the CRS attributes are known at the reference trace (located at midpoint $m = 0$). However, it could be helpful in practice to decompose the calculation into the three steps below. The reason is that we shall make use later of the calculated values obtained in the individual steps.

(i) First, we evaluate $t(0, h)$, the time of the chosen event within the CMP gather, at half-offset h. In the 2-D case, this is obtained setting $m = 0$ in eq. (2), namely

$$t^2(0, h) = t^2(0, 0) + P_3 h^2. \tag{5}$$

(ii) Second, we evaluate $t(m, 0)$, the traveltime of the chosen event within the ZO section, at midpoint m. In the 2-D case, this is obtained setting $h = 0$ in eq. (2), namely

$$t^2(m, 0) = (t(0, 0) + P_1 m)^2 + P_2 m^2. \quad (6)$$

(iii) Finally, we evaluate $t(m, h)$, the traveltime for the same event at midpoint m and half-offset h. This can be achieved by means of the equation

$$t^2(m, h) = t^2(m, 0) + t^2(0, h) - t^2(0, 0), \quad (7)$$

which combines the previous two results.

This final eq. (7) reveals how the hyperbolic traveltime of a reflection event at any midpoint and offset can be simply derived from the ones that refer to the ZO and CMP gathers. It can be seen as a decomposition of the traveltime squared $t^2(m, h)$ in terms of the squared ZO and CMP traveltimes, $t^2(m, 0)$ and $t^2(0, h)$, respectively. It is valid as long as the CRS traveltime approximation is. For example, it is exact for a dipping plane reflector with a homogeneous overburden.

We remark that a similar decomposition formula, using, however, traveltimes instead of traveltimes squared, have been presented in Tygel & Santos (2006), but it is valid in a shorter range.

2.2 Equation for amplitude

Although it has been relatively straightforward to predict the traveltime above, this is not the case with amplitude. This is so because the CRS stack method provides kinematic attributes only. As a matter of fact, full account of amplitudes involves many factors, such as angle-dependent reflection/transmission coefficients, geometrical spreading, medium attenuation, source wavelet etc. Determination of all these quantities is, of course, unfeasible. Nevertheless, as shown below, a reasonable approximation can be achieved. Our idea is similar to the one presented in a previous work by Rousset *et al.* (2001), that is to rely on the available data itself to estimate amplitudes.

We suppose we have full knowledge (traveltime and amplitude) at each sample of the two specific ZO and CMP gathers. More specifically, we consider that for each event that we select, the traveltime and amplitude pairs $[t(0, m), A(0, m)]$ and $[t(0, h), A(0, h)]$ that refer to the ZO and CMP gathers, respectively, are known. Note that, for the determination of the traveltime $t(m, h)$, we have already computed, with the help of the eqs (5) and (6), the traveltimes $t(m, 0)$ and $t(0, h)$. We can therefore pick the corresponding amplitudes $A(m, 0)$ and $A(0, h)$ within the given ZO and CMP gathers, together with the amplitude $A(0, 0)$ at time $t(0, 0)$ at the reference trace (see Fig. 1). The question now is how to evaluate the unknown amplitude $A(m, h)$ relatively to these known (data-driven) quantities.

Our main assumption is that the predicted traveltime, $t(m, h)$, and amplitude, $A(m, h)$, are supposed to be valid only in the neighbourhood around the reference trace, so the CRS traveltime equation should provide a good approximation. Concerning the amplitude, we further assume that the physical quantities such as velocities, densities, are also more or less stationary in this neighbourhood. As a consequence, we may restrict the analysis to the main laterally variable factors, which are geometrical spreading and reflection angle. We propose here that the change of amplitude with offset (AVO effect) can be considered stationary with respect to midpoint variation. In this way, after estimating the amplitude change with offset at the reference point from the known CMP gather, we can use it as an estimate for amplitude change with offset for neighbouring midpoints.

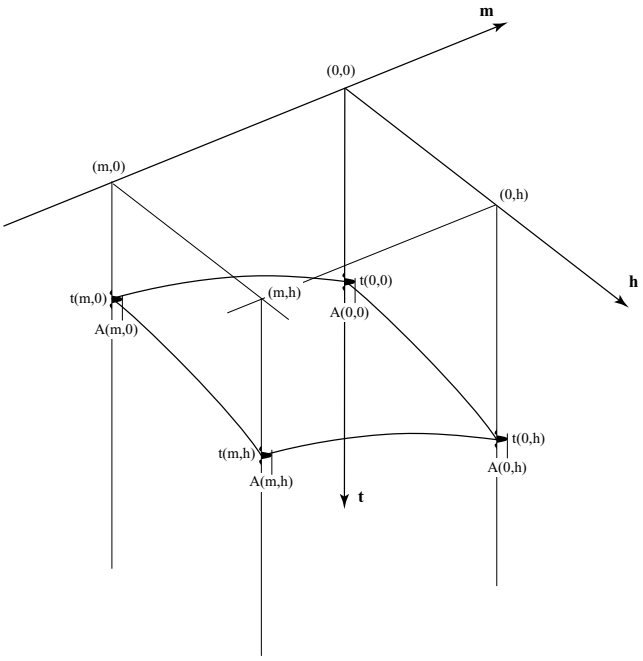

Figure 1. Schematic representation of quantities used in the calculation.

As the depth of the reflector can change laterally, it is clear that both the geometrical spreading and reflection angle can significantly change. In accordance, the changes in amplitude introduced by these two factors are investigated below (see Appendix A for a detailed derivation).

(i) **Geometrical spreading:** As well known (see, e.g. Tygel *et al.* 1992; Červený 2001), the precise evaluation of geometrical spreading can be a complicated task, with factors such as source and receiver ray angles, as well as second mixed derivatives of traveltime with respect of source and receiver coordinates. Once again, our goal here is to evaluate only the local change in geometrical spreading, in a 'small' area where the Earth subsurface is supposed to have stationary parameters. In this situation, we propose to approximate the change of geometrical spreading in terms of the variations in traveltime. More precisely, we will consider the change of amplitude as a function of the quantity $t^\alpha(m, h)$, namely the traveltime to the power α, where $\alpha = 1/2$ for the case of 2-D in-plane spreading only and $\alpha = 1$ in the case of 3-D spreading. We note, in particular, that for a planar dipping reflector in 2-D with a homogeneous overburden, the geometrical spreading factor is exactly $t^{1/2}(m, h)$. As a consequence, the amplitude after geometrical spreading correction reads $A(m, h) \times t^{1/2}(m, h)$.

From the above observations, we propose that, instead of trying to estimate the change in amplitudes, $A(m, h)$, we consider the change of the quantity $A(m, h) \times t^\alpha(m, h)$. In the seismic literature, that quantity is known as a *true amplitude* (see, e.g. Schleicher *et al.* 2007).

(ii) **Reflection angle:** As the depth of the reflection point can vary with midpoint m, it implies that for a given half-offset h, the reflection angle, θ, can also vary with the reflection-time $t(m, h)$. Shuey (1985) has provided a useful approximation for the relative change with angle of the reflection coefficient, and therefore amplitude, that can be written in the form

$$R(\theta) - R(0) = G \sin^2(\theta), \quad (8)$$

where $R(\theta)$ stands for the reflection coefficient as a function of the reflection angle, θ, and G is a constant that depends on the local physical parameters only. For our purposes, we can consider G as a constant in the neighbourhood of the reference trace. Thus, the relative variation (ratio) of the reflection coefficient at any midpoint, m, with respect to the reflection coefficient at the reference midpoint can be simply approximated by the corresponding variation (ratio) of $\sin^2(\theta)$ at these two midpoints. We note, in particular, that for our familiar example of a planar dipping reflector in a 2-D homogeneous overburden, this ratio can be shown to be equal to the ratio between squared traveltimes (see Appendix A).

Based on the above considerations, we propose to replace the variation of the quantity $R(\theta) - R(0)$ between midpoint m and the reference midpoint by the quantity $t^2(0, h)/t^2(m, h)$.

(iii) **Final amplitude equation:** The two above considerations lead to the following equation to evaluate the amplitude at position, m, and half-offset, h,

$$A(m,h) = \frac{1}{t^{\alpha}(m,h)}\left\{A(m,0)t^{\alpha}(m,0) + \frac{t^2(0,h)}{t^2(m,h)}\left[A(0,h)t^{\alpha}(0,h) - A(0,0)t^{\alpha}(0,0)\right]\right\}. \quad (9)$$

Note that this formula leaves unchanged the amplitude within the ZO gather ($h = 0$), as well as within the CMP gather ($m = 0$).

The evaluation of the unknown quantity, $A(m, h)$, relies only on quantities that are data-dependent, which can be picked from the two given specific configurations or computed from the CRS attributes. No other information is required, as long as the stationarity of model physical parameters in the vicinity of the reference position is a valid approximation. This process can therefore really be qualified as data-driven and macro-model-independent.

2.3 General algorithm

We shall now assemble the above obtained results as building blocks of an algorithm that will produce a new data record at midpoint position, m, and half-offset, h, starting from the given ZO and CMP gathers in the neighbourhood of the reference trace.

(1) First, if not known, compute the CRS attributes for all samples of the record at the reference position ($m = 0$). For that, use the CMP gather (to obtain P_3 in the 2-D case), and the ZO gather (to obtain P_1 and P_2 in the 2-D case), together with the corresponding coherence values. This has to be done only once for all data traces to be built in the vicinity of the given reference trace.

(2) Start a loop on time samples, $t(0, 0)$, with amplitude, $A(0, 0)$, from the record at the reference midpoint, $m = 0$, and half-offset, $h = 0$. Each time sample will be taken as a possible reflection event if its CRS attributes have coherence values that are high enough. Otherwise, go to the next sample.

(i) Compute $t(0, h)$, $t(m, 0)$ and $t(m, h)$ from $t(0, 0)$ and its CRS attributes, according to eqs (5–7).

(ii) Pick $A(0, h)$ at time $t(0, h)$ in the CMP gather and $A(m, 0)$ at time $t(m, 0)$ in the ZO gather, using interpolation from surrounding data samples, and compute $A(m, h)$ using eq. (9).

(iii) All obtained pairs of time and amplitude should be stored for future use. Note that calculated times are not necessary monotonously increasing. In the case there are more than one group of CRS attributes for the same time sample (conflicting dips), this process has to be carried out for each CRS attribute group.

(3) End of the loop on time samples.

(4) Order the time-amplitude pairs by increasing times and interpolate the amplitudes at the data time-sampling rate.

The above algorithm, which builds a single data trace, can then be used in a loop on midpoint, m, and fixed half-offset, h, to build a common-offset (CO) section. In addition, in an outer loop on half-offset, h, it can be further used to build the full data set.

Note that with this scheme, a given reflection event is built sample by sample, so that we do not have to make any assumptions on the signal wavelet, only that it has been adequately sampled. Preprocessing steps such as filtering or deconvolution that enhance the signal-to-noise ratio and signal resolution can be applied on the ZO and CMP gathers. This can be done either before or after the application of the algorithm.

3 SYNTHETIC EXAMPLES

The synthetic data have been computed by a ray tracing calculation with 2-D in-plane amplitudes, convolution by a ricker wavelet and addition of white noise with a signal-to-noise ratio of 10.

Two simple models will be tested to check the efficiency of our algorithm. They are shown in Fig. 2. The models consist of (1) a dipping planar reflector, within a homogeneous overburden, for which the time eq. (7) is exact, and (2) a circular reflector, tangent to the dipping plane at the normal incidence point for the reference position, for which the time eq. (7) is only approximate. The choice of these models reflects our assumption that the Earth subsurface has to be locally simple enough so that the CRS traveltime equation provides a good approximation.

3.1 Dipping plane

Fig. 3(a) shows the two specific configurations that have been used to build the full data set: the ZO gather on the top and the CMP gather at the bottom. From the traces in these two gathers, the CRS attributes at the reference midpoint $m = 0$ have been extracted,

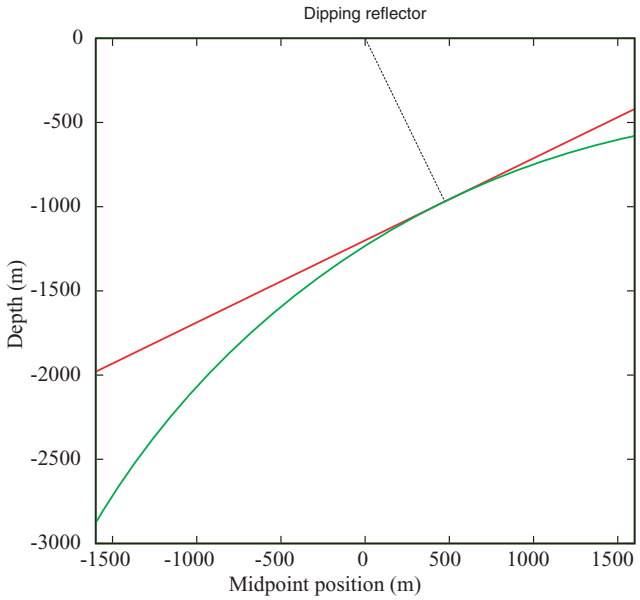

Figure 2. Simple synthetic examples: the red line represents the dipping planar reflector, the green line the circular reflector and the black line the common normal ray; both reflectors are tangent at the normal incidence point.

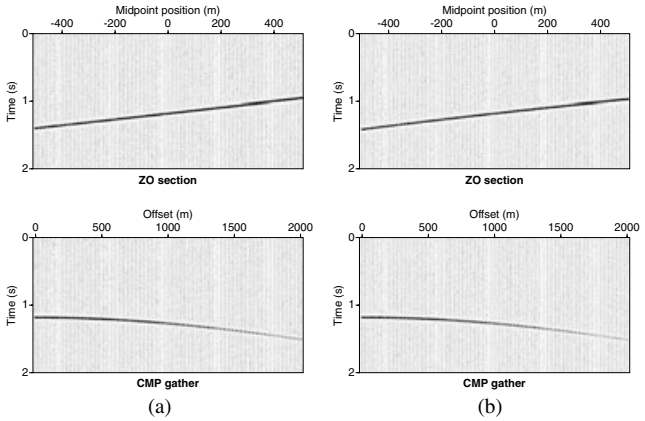

Figure 3. Synthetic data for (a) the planar dipping reflector and (b) the circular reflector.

together with their coherence values. They are shown at Fig. 4(a). Traces were then built following the above-described algorithm for all midpoints and offsets. The built traces are compared to the synthetic data in Fig. 5(a), for small, medium and large offsets. We can see how the built trace compares well with the synthetic data in the vicinity of the reference midpoint, but differences appear when offset or distance to the reference midpoint increase. To evaluate how far we can go, a map of the relative mean quadratic error is shown in Fig. 6(a). The contour at 0.2 provides a conservative estimation of the area where the approximation is very satisfying. It covers an extent approximately equal to the reflector depth, both in the offset and midpoint direction. Note that the noise is suppressed by the process when there is no coherent signal, that is when CRS-attribute coherency is less than a given threshold.

3.2 Circular reflector

The same figures (Figs 3b to 6b) were obtained for the circular reflector. Note that in this case, the CRS traveltime formula is only approximate, so the differences between the built traces and the synthetic data become significant for shorter offsets, or distances from the reference midpoint.

However, there further exists a significant range where the differences between the synthetic data and the data built with the Inverse CRS algorithm can be considered negligible. Its width, both in midpoint and offset coordinates, is approximately equal to the target depth in these simple cases (about 1000 m). To check how the algorithm behaves in more complex situations, an illustration has been performed using real data.

3.3 Real data set

To test the Inverse CRS algorithm in a real data case, we present an application for interpolating missing traces in a near-surface high-resolution seismic experiment, conducted in the alluvial plain of the river Gave de Pau, near Assat, southern France. As shown by the stack section obtained after conventional processing (Fig. 7), the subsurface consists in a pile of horizontal depositional layers, with clear impedance contrasts at various times in the range 0.03–0.14 s, corresponding to depths between 30–150 m for an average velocity around 2000 m s^{-1}. The data were obtained using 1 m spacing for both shots and receivers, and offsets in the range 0–70 m. To increase the CMP fold, neighbouring CMP gathers were mixed 2 by 2, so the CMP interval is also 1 m. This stack section will be used here

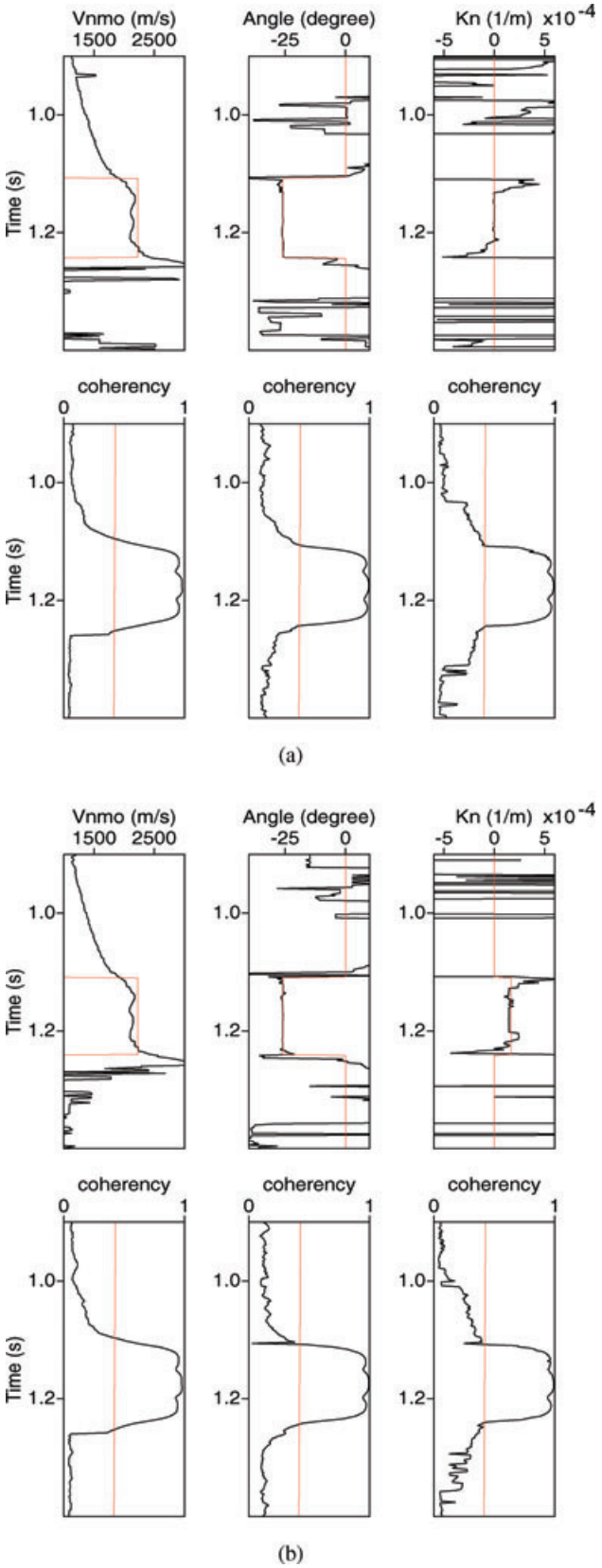

Figure 4. CRS attributes and their corresponding coherency obtained from the reference position for (a) the planar dipping reflector and (b) the circular reflector. In both figures, the expected attribute value in its validity range is also shown in red. The red line on coherency plots represents the coherency threshold for acceptance of attributes values.

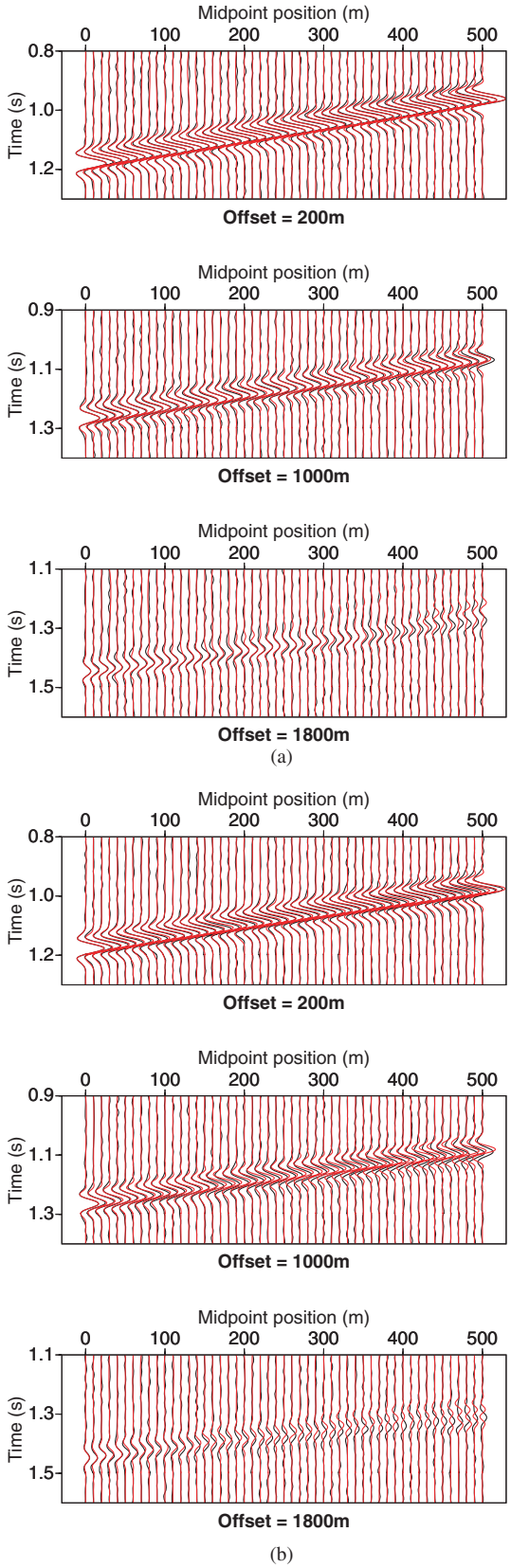

Figure 5. Comparison of the built traces (in red) with the synthetic data (in black) for small, medium and large offsets, with the reference midpoint located at position 0. (a) Planar dipping reflector; (b) Circular reflector.

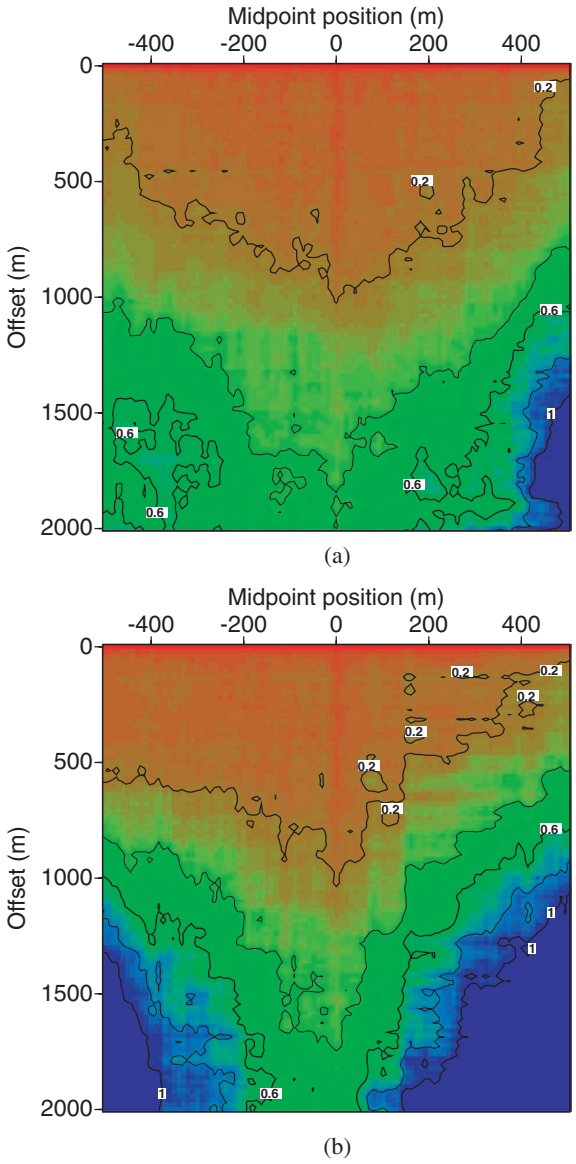

Figure 6. Map of the relative mean quadratic error introduced by the process: (a) Planar dipping reflector; (b) Circular reflector.

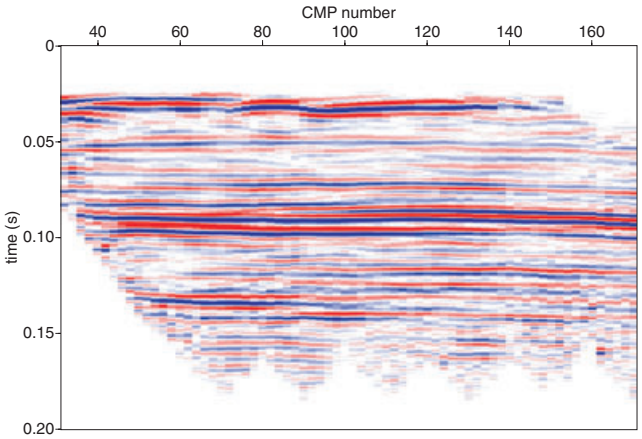

Figure 7. Conventional stack section, used here as the reference ZO section.

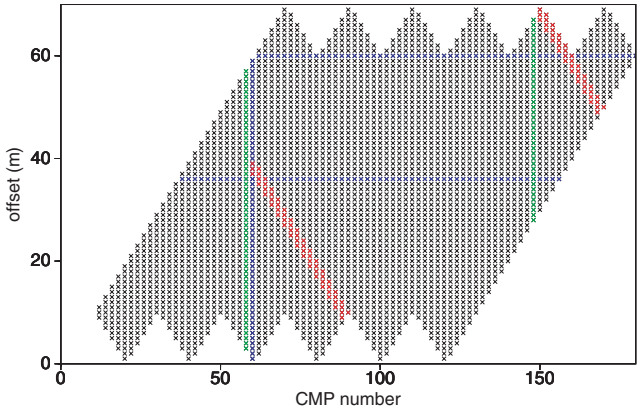

Figure 8. Acquisition map in the offset-CMP coordinates, with missing traces in red, reference CMP gathers in green and the gathers to be built in blue.

as our best estimate of the ZO section needed by the Inverse CRS algorithm.

The seismic acquisition experiment was conducted using a set of two-channel DMT Summit boxes connected by a wire to the control unit. It appeared that one of the boxes was not working properly, so that the corresponding traces were killed for further processing. These missing traces are located in red in the acquisition map of Fig. 8. Our purpose here will be to apply the Inverse CRS algorithm to build replacement traces, to avoid the processing artefacts generated by such discontinuities.

Trace interpolation for seismic data has long been a topic of research, since the seismic data migration algorithms generally assume unaliased regular spatial sampling, what is not always possible to achieve during data acquisition, due to real world physical or economic constraints. Classically, it is achieved by linear-event extrapolation in the time–space domain (Bardan 1987) or in the frequency–space domain (Spitz 1991). We propose here a different data-driven approach based on CRS attributes, that does not need to make assumptions about the linearity of seismic events. Another CRS-based approach (Hoecht *et al.* 2009) was proposed recently as an operator-oriented interpolation scheme, that is more intended at regularize irregular data geometry, looking for coherencies in common-offset volumes. We feel that our approaches are complementary, since our interpolation scheme can be used from sparse data only.

To apply the Inverse CRS algorithm, reference CMP gathers have to be chosen in the vicinity of the traces to be built. The CMP gathers corresponding to CMP number 58 and 148 were chosen as reference CMP for Inverse CRS application. These gathers are shown in Fig. 9, and their locations with respect to missing traces are shown in Fig. 8.

We present here the results corresponding to a set of demonstration gathers, which are shown in blue in Fig. 8. The first one is the CMP gather corresponding to the CMP number 60, where three traces are missing. Next, two common offset gathers (COG) have been processed, corresponding to intermediate (36 m) and large (60 m) offsets. Two traces are missing in each of these gathers. The demonstration gathers are shown in Fig. 10, with available traces in black. Note that noisy parts of the traces were muted both above and below the reflection events, to eliminate unwanted signals, such as refracted *P*-waves, or direct surface waves.

For the different demonstration gathers, the new traces obtained using the Inverse CRS algorithm are shown in red in Fig. 10, and

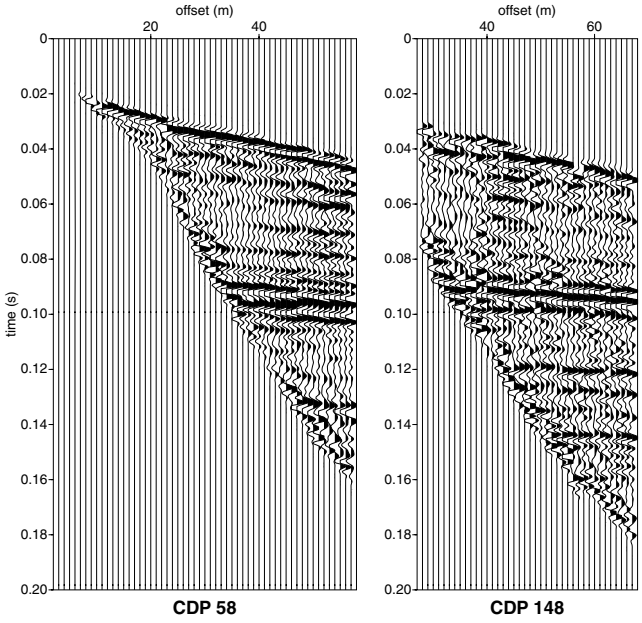

Figure 9. Reference CMP gathers chosen to build the missing traces.

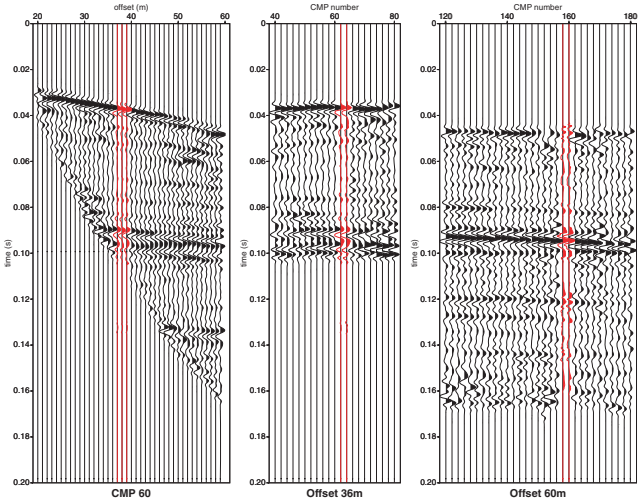

Figure 10. Results of the Inverse CRS traces building: the interpolated traces in red are compared with the normally acquired traces in black.

compared with their normally acquired neighbouring traces in black. In most cases, the results look very satisfying, especially when the offset is not too large. However, a few artefacts seem to appear in the COG 60 m: at the beginning of the unmuted zone, the offset is much larger than the target depth, so we should not expect the Inverse CRS approximations to be valid; at the end of the trace, the increase of the noise level seems to be responsible for the observed discrepancies. A somewhat unexpected good feature of the algorithm, is that it seems capable to reconstruct signals even in muted part of the section. This can be seen by the event around 0.14 s, visible on the constructed traces, both in the CMP gather 60 and the COG gather 36 m.

4 CONCLUSIONS

At the present stage of this on-going research, we have proposed an algorithm that is able to build seismic traces from a very limited set of real data, namely a CMP gather and a ZO section, together with

the CRS attributes that can be obtained from them. First synthetic tests of the algorithm provide satisfying results for the two simple cases of single dipping plane and singular circular reflectors with a homogeneous overburden. The region of accepted approximations has been observed to be, in midpoint and offset, of a similar extent as the reflector depth in the first case, and a little less in the second case. Further tests carried out with real seismic data have also given positive results, showing the ability of the proposed algorithm to interpolate missing traces. In principle, the technique could be extended to larger offset ranges in 2-D by the use of Common-Offset CRS stack method, and could also be adapted to 3-D using the 3-D ZO CRS stack method. Applications of this technique could be numerous, from noise suppression, data compaction, trace interpolation, etc.

ACKNOWLEDGMENTS

This research was initiated during the sabbatical stay of H.P. at the Laboratory of Computational Geophysics, State University of Campinas, Brazil, with the support of the Research Foundation of the State of São Paulo, Brazil. We acknowledge support of the National Council of Scientific and Technological Development (CNPq-Brazil) and from the sponsors of the WIT Consortium.

REFERENCES

Bardan, V., 1987. Trace interpolation in seismic data processing, *Geophys. Prospect.,* **35,** 343–358.

Červený, V., 2001. *Seismic Ray Theory,* Cambridge University Press, Cambridge.

Della-Moretta, D., Klüver, T. & Marchetti, P., 2001. 3D CRS-based velocity model building: an accurate and cost-effective approach, in *Proccedings of the 8th EAGE Conference and Exhibition,* Vienna.

Hertweck, T., Schleicher, J. & Mann, J., 2007. Data stacking beyond CMP, *Leading Edge,* **7,** 818–827.

Hoecht, G., Ricarte, P., Bergler, S. & Landa, E., 2009. Operator-oriented CRS interpolation, *Geophys. Prospect.,* **57,** 957–979.

Hubral, P., 1983. Computing true-amplitude reflections in a laterally inhomogeneous earth, *Geophysics,* **48,** 1051–1062.

Hubral, P., 1999. Special issue: macro-model independent seismic reflection imaging, *J. appl. Geophys.,* **42,** Nos. 3,4.

Jäger, R., Mann, J., Höcht, G. & Hubral, P., 2001. Common reflection surface stack: image and attributes, *Geophysics,* **66,** 97–109.

Klüver, T., 2006. Velocity model building using migration to residual time, in *Proceedings of the 76th SEG Annual Meeting,* Extended Abstracts, New Orleans, USA.

Koglin, I., Mann, J. & Heilmann, Z., 2006. CRS-stack-based residual static correction, *Geophys. Prospect.,* **54,** 697–707.

Perroud, H. & Tygel, M., 2005. Velocity estimation by the common-reflection-surface (CRS) method: using ground-penetrating radar data, *Geophysics,* **70,** B43–B52.

Prüssmann, J., Tygel, M., Gamboa, F. & Coman, R., 2006. Multiple suppression by the CRS technique. *GEO 2006,* Bahrain.

Rousset, D., Tygel, M. & Perroud, H., 2001. Attaching true amplitude to kinematically migrated images, *J. seism. Expl.,* **10,** 149–184.

Schleicher, J., Tygel, M. & Hubral, P., 2007. *True Amplitude Seismic Imaging,* Society of Exploration Geophysics (SEG), Tulsa.

Shuey, R.T., 1985. A simplification of the Zoeppritz equations, *Geophysics,* **50,** 609–614.

Spitz, S., 1991. Seismic trace interpolation in the F-X domain, *Geophysics,* **56,** 785–794.

Tygel, M. & Santos, L.T., 2006. Quadratic normal moveouts of symmetric waves in elastic media: a quick tutorial, *Studia Geophysica et Geodetica,* **51,** 185–206.

Tygel, M., Schleicher, J. & Hubral, P., 1992. Geometrical spreading corrections of offset reflections in a laterally inhomogeneous earth, *Geophysics,* **57,** 1054–1063.

Yilmaz, O., 2000. *Seismic Data Analysis,* Vol. 1, Soc. of Expl. Geophys, Tulsa, OK.

APPENDIX A: DERIVATION OF AMPLITUDE EQUATION

Here we derive eq. (9), which was used to construct the amplitudes, $A(m, h)$, as a function of the traveltimes and amplitudes of the ZO section and reference CMP gather.

Our derivation assumes that the amplitude to be reconstructed belongs to a primary reflection. In accordance to small offset and midpoint variations, we use zero-order ray theory, to express the amplitude as the proportionality relation

$$A(m,h) \propto \frac{R(m,h)}{\mathcal{L}(m,h)}\,, \tag{A1}$$

in which $R(m, h)$ is the reflection coefficient and $\mathcal{L}(m, h)$ is the geometric spreading. The latter, moreover, is assumed to be proportional to traveltime, namely

$$\mathcal{L}(m,h) \propto t^{\alpha}(m,h)\,, \tag{A2}$$

where $\alpha = 1/2$ or $\alpha = 1$ in the 2-D and 3-D situations, respectively. The above two relations can be recast into the single equation

$$A(m,h) = C\frac{R(m,h)}{t^{\alpha}(m,h)}\,, \tag{A3}$$

in which C denotes a constant. Our next step is now to find a suitable approximation for the reflection coefficient, $R(m, h)$. The simplest one is Shuey's approximation (Shuey 1985)

$$R(m,h) = R(m,0) + G\sin^2\theta(m,h)\,, \tag{A4}$$

where the $R(m, 0)$ and G are the so-called intercept and gradient, respectively, and $\theta(m, h)$ is the incidence angle of the reflection ray at the reflection point. In the framework of small midpoint variation, we assume that G is independent of m.

We now make use of Fig. A1 to approximate $\sin\theta(m, h)$ as

$$\sin\theta(m,h) = \frac{2h\cos\gamma}{vt(m,h)}\,, \tag{A5}$$

in which v is an 'average' (constant) velocity and γ is the reflector dip, whose cosine variations could be considered as negligible for

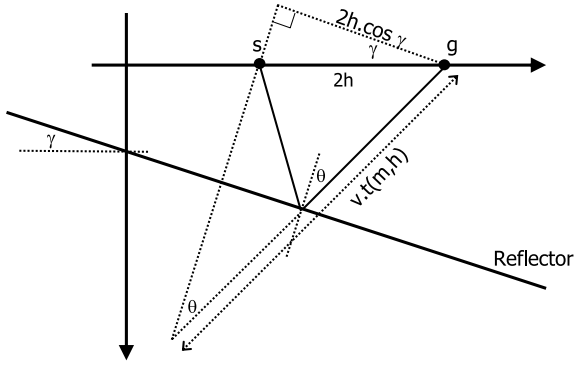

Figure A1. Geometry for the approximation formula for $\sin\theta(m, h)$. The reflector is assumed planar with dip γ. Overburden is homogeneous with an average velocity v.

small variations of m. Multiplying both sides of Shuey's eq. (A4) by C and using eq. (A3) twice to replace $CR(m, h)$ and $CR(m, 0)$, respectively, we can write

$$A(m, h)t^{\alpha}(m, h) - A(m, 0)t^{\alpha}(m, 0) = C.G \sin^2\theta(m, h),$$
$$A(0, h)t^{\alpha}(0, h) - A(0, 0)t^{\alpha}(0, 0) = C.G \sin^2\theta(0, h). \quad \text{(A6)}$$

Division of both the above equations together with the use of eq. (A5) yields

$$\frac{A(m, h)t^{\alpha}(m, h) - A(m, 0)t^{\alpha}(m, 0)}{A(0, h)t^{\alpha}(0, h) - A(0, 0)t^{\alpha}(0, 0)} = \frac{t^2(0, h)}{t^2(m, h)}\,. \quad \text{(A7)}$$

Rearranging the above equation to have $A(m, h)$ explicit, we recover the amplitude eq. (9) given in the text.